Affiliates Program Meeting 2023
November 8th, 2023

Trajectory Informed Multi-fidelity Surrogates for Hypersonic Vehicle Optimization

Jacob Needels (PhD Candidate), Prof. Juan J. Alonso

There is always a trade between **accuracy** and **computational cost** in aircraft design, particularly for hypersonic vehicles

Uncertainties and/or biases in conceptual design tools can result in **risk to performance and closure** in later design stages

Multi-fidelity methods can **"correct" low-fidelity models** using a **small number** of high-fidelity samples, to improve accuracy for minimal cost

We focus on **improving the information state in conceptual design** while maintaining **tractable computational cost** through:

- **Multi-fidelity Gaussian Process surrogates** of aerodynamic/aerothermal loads, incorporating **model uncertainties**
- **Adjoint-based sensitivity analysis** to guide **sampling** and improve surrogate accuracy for mission-based objectives
- Multidisciplinary **vehicle-trajectory co-design and optimization**

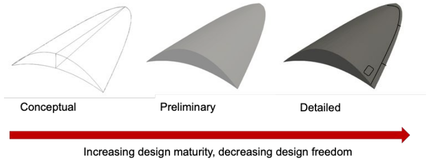

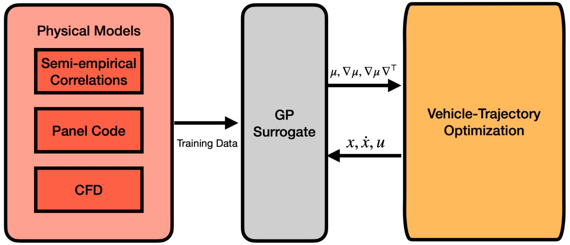

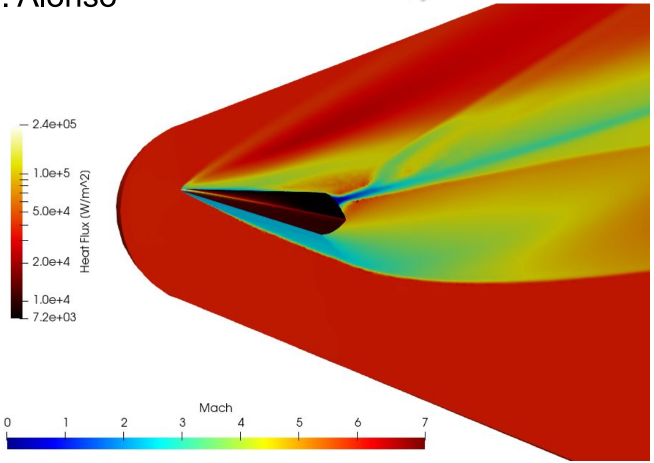

Panel Code

CFD

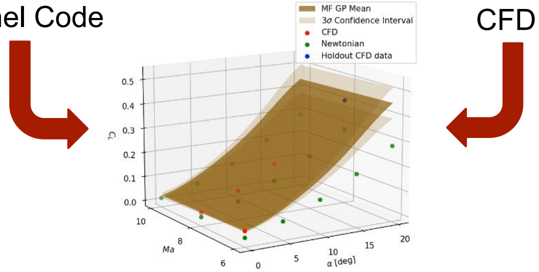

Multi-fidelity Gaussian Process

Model	Fidelity	Uncertainty	Cost
SU2	High	$\pm 4\%$	$\mathcal{O}$(cpu-hour)
SHARPE	Low	$\pm 20\%$	$\approx$ 1 cpu-sec

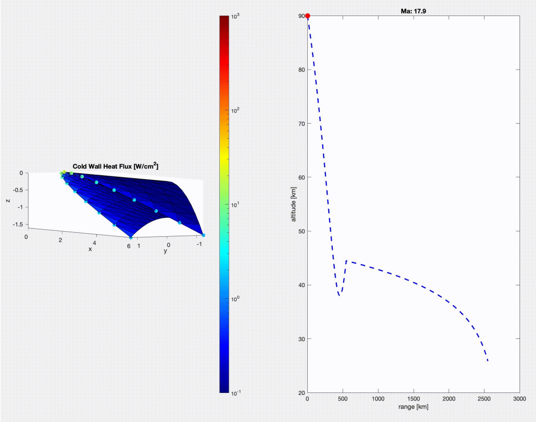

$\mu, \nabla\mu, \ \ldots \sim \mathcal{GP}(m, k)$

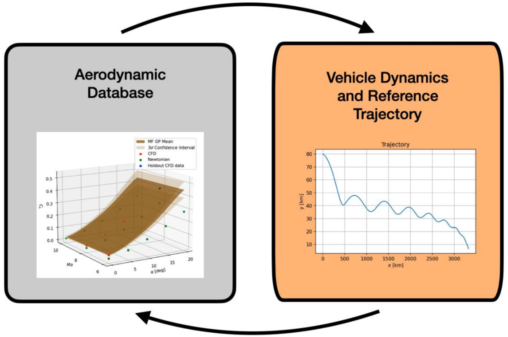

$\delta J = \lambda^T R(x_{ss}, A + \delta A)\delta t$

Adjoint-based trajectory sensitivities inform sampling

SACL

Fly-By-Feel: Bio-Inspired Flight Awareness via Distributed Sensing

Bio-Inspired Sensing

Distributed Nerve Endings

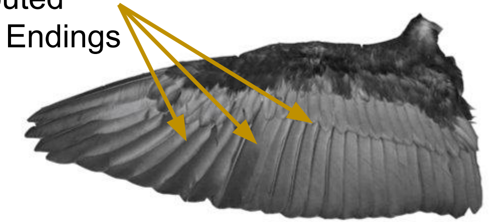

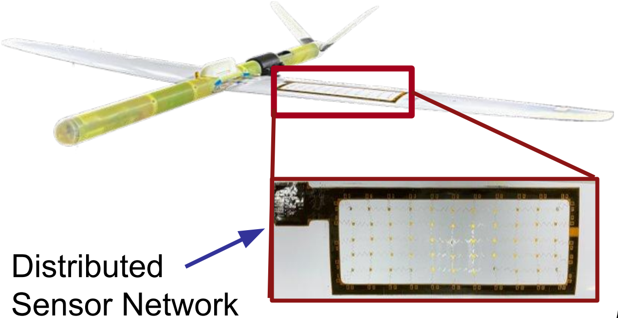

Distributed Sensor Network

Biology

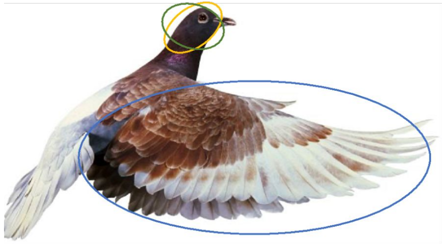

Fly-by-feel Aircraft

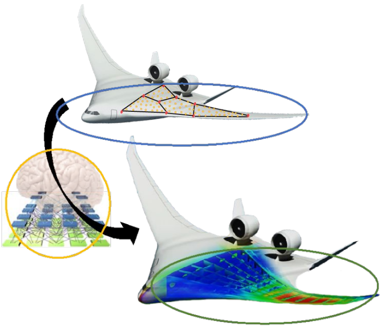

Bio-Inspired State Perception

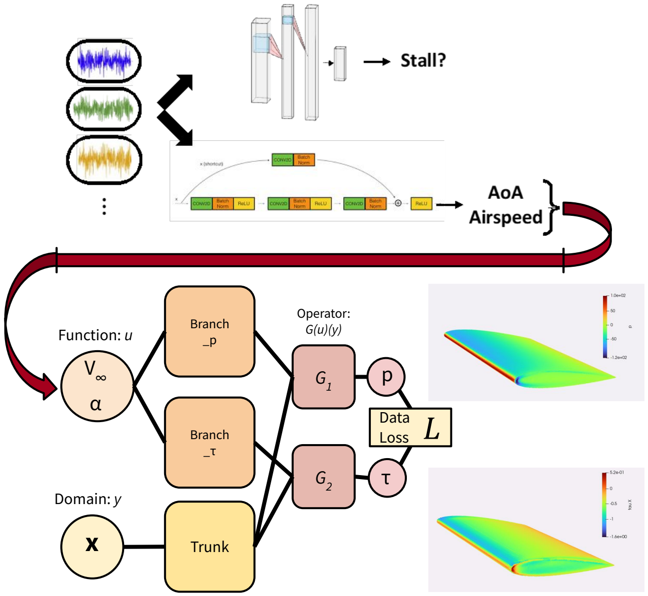

Neural Methods for Processing Sensor Data

An Interdisciplinary Investigation of Hypervelocity Impact Plasmas

<u>Nancy Diallo</u> (PhD Student), Raymond Lau (PhD Candidate), Dr. Nicolas Lee, and Prof. Sigrid Elschot

Figure 1: Depiction of HVI Plasma Expansion Process

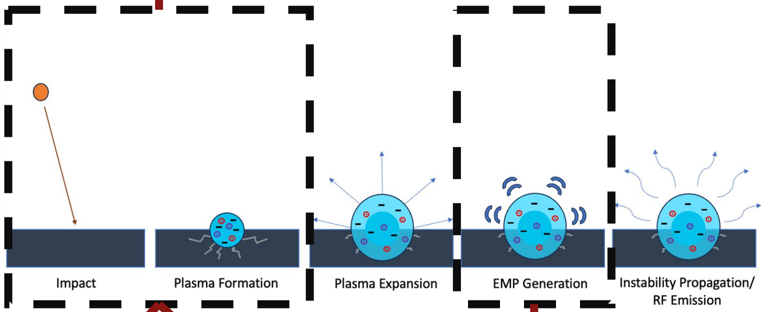

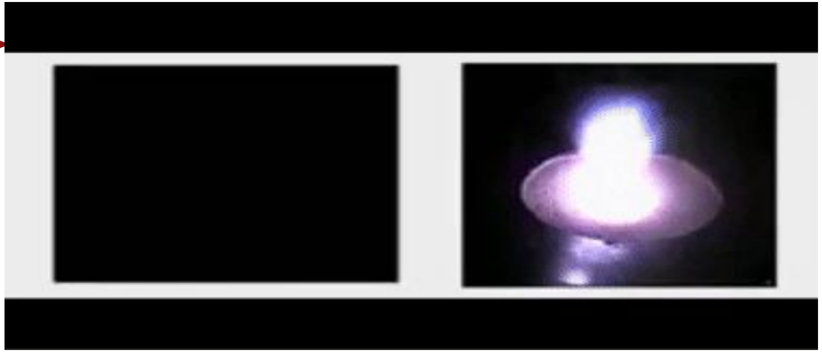

Figure 2: Optical flashes from projectile impacts on a metallic target

Figure 3: Charge density ρ, Electric fields E_x and E_y, and magnetic field B_z

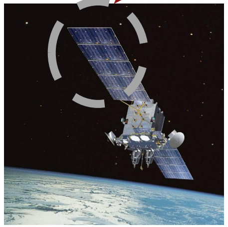

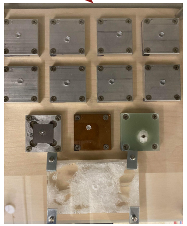

Figure 4: Damaged Targets from HVI Experiments

Marie-Jo Azzi

PhD Candidate

Farhat Research Group (FRG)

Advisor: Charbel Farhat

Physics-Based Digital Twins of Engineering Systems

Marie Jo Azzi[1], Charbel Farhat[1, 2, 3]

Department of Mechanical Engineering, Stanford University

Department of Aeronautics and Astronautics, Stanford University

Institute for Computational Mathematics and Engineering, Stanford University

What is a Digital Twin?

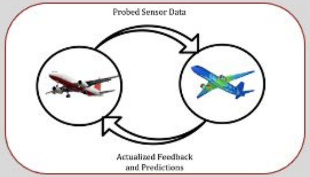

- **Digital twin prototype (DTP)**

Replica of a physical asset/system before it is manufactured. Serves design/analysis purposes .

- **Digital twin instance (DTI)**

Replica of a physical asset/system after it has been manufactured.
Updated in real time to assist with operations (e.g. predictive maintenance.) .

Surrogate Models: Internal vs External

- **External models (data-driven)**

Few, pre-determined*, scalar quantities of interest (QoIs).
Real-time, surrogate models of output (s).
Gaussian processes, artificial neural networks, ...

- **Internal models (physics-based)**

Arbitrary number of scalar and vector QoIs that can be discovered using the constructed surrogate model.
Real-time, surrogate model of system.
Projection-based reduced-order models

***How to identify the QoIs (rare events, failure modes, ...)?**

Model-Form Uncertainty (MFU)

- **MFU inherent to computational model**

Lack of knowledge of the true physics underlying the problem of interest.
Omission or truncation of modeling details.

- **MFU inherent to surrogate model**

Typical methods for UQ involve stochastic computations (e.g. Monte Carlo realizations).
Surrogate models typically adopted to achieve computational tractability → additional MFU

Requirements for a DT

- **High-fidelity modeling**, whether data-driven or physics-based.
- **Modeling and quantifying uncertainty,** and particularly those due to both aforementioned sources of MFU
- **Model Updating,** using a nonparametric stochastic approach.

Key Performance Indicators

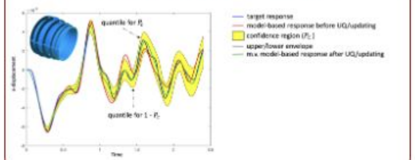

NPM for Modeling and Quantifying MFU

NPM randomizes the subspace in which the solution is approximated:

- Operates at the level of the HPROM instead of that of the HDM to achieve computational tractability.
- Substitutes the deterministic ROB V with a stochastic counterpart $\mathbf{V}(\alpha)$, where α is a vector-valued hyperparameter → hyperparametrized ROB and HPROM.

Desired properties of the stochastic ROB:

- $\mathbf{V}(\alpha)$ is global.
- $\mathbf{V}(\alpha)$ is random with a probability distribution constructed using MaxEnt.
- Linear independence of the column is enforced by ensuring that $\mathbf{V}^T(\alpha)Q\mathbf{V}(\alpha) = I$

→ NPM constructs the probability measure of $\mathbf{V}(\alpha)$ on a compact Stiefel manifold

- Enrichment with data via inverse statistical problem
- Identification of hyperparameter vector α

$$\alpha^{opt} = \arg\min_{\alpha} J(\alpha)$$

$$J(\alpha) = w_m J_{mean}(\alpha) + w_s J_{std}(\alpha) + (1 - w_m - w_s) J_{orth}(\alpha)$$

$$w_m \geq 0, w_s \geq 0, (w_m + w_s) \leq 1$$

$$J_{mean}(\alpha) = \sum_{k=1}^{n_p} \sum_{j=1}^{n_o} \frac{1}{c^j_{mean}(\varrho_k)} d\left(o_j^{ref}(\varrho_k), E[\mathbf{o}_j(\varrho_k, \alpha)]\right)$$

$$J_{orth}(\alpha) = E\left(\|(I - \mathbf{V}(\alpha)\mathbf{V}^T(\alpha)) u^{HDM}\|^2\right)$$

- ϱ_k: specified model parameter
- o_j^{ref}: observable from target data
- $\mathbf{o}_j$: observable from stochastic HPROM

SHPROM

$$\mathbf{M}_r(\alpha)\ddot{\mathbf{y}}(t,\alpha) - \tilde{\mathbf{f}}_r^{int}(\mathbf{y}(t,\alpha)) = \tilde{\mathbf{f}}_r^{ext}(t,\alpha)$$

$$\mathbf{M}_r(\alpha) = \mathbf{V}^T(\alpha)M(\mu)\mathbf{V}(\alpha)$$

$$\tilde{\mathbf{f}}_r^{int}(\mathbf{y}(t,\alpha)) = \sum_{e \in \tilde{\mathcal{E}} \subset \mathcal{E}} \xi^e (L^e\mathbf{V}(\alpha))^T f^{int^e}(L^e\mathbf{V}\mathbf{y}(t,\alpha))$$

$$\tilde{\mathbf{f}}_r^{ext}(t,\alpha) = \sum_{e \in \tilde{\mathcal{E}} \subset \mathcal{E}} \xi^e (L^e\mathbf{V}(\alpha))^T f^{ext^e}(t)$$

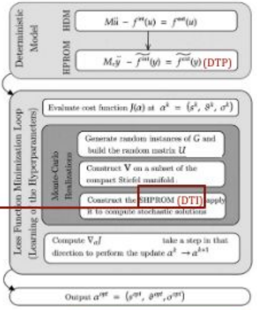

Structural Health Monitoring

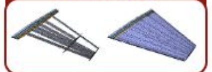

Results

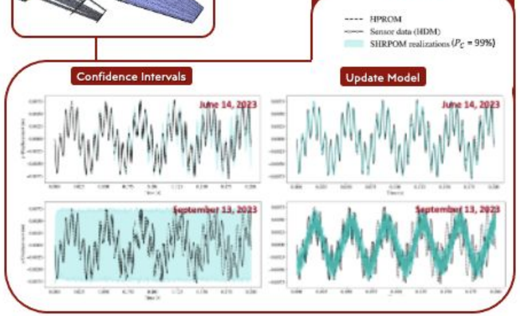

References

- Soize, C., & Farhat, C. (2017). A Nonparametric Probabilistic Approach for Quantifying Uncertainties in Low-dimensional and High-dimensional Nonlinear Models. International Journal For Numerical Methods In Engineering, 109(6), 837-888.
- Azzi, M. J., Ghnatios, C., Avery, P., & Farhat, C. (2023). Acceleration of a Physics-Based Machine Learning Approach for Modeling and Quantifying Model-Form Uncertainties and Performing Model Updating. Journal of Computing and Information Science in Engineering, 23(1), 011009.

Satellite Ephemeris Parameterization for Lunar PNT

Marta Cortinovis, Keidai Iiyama, and Grace Gao

Background

Increasing international interest in providing communication and navigation services in the lunar regime via satellite constellations.

Objective

Develop **satellite ephemeris approximation methods** compliant with system requirements

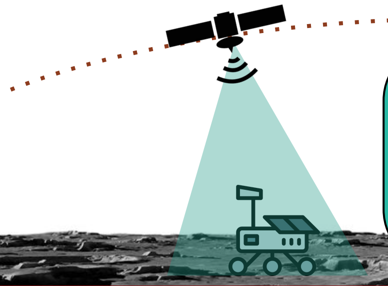

Broadcasted parameters considered

➔ Sat Position

➔ Sat Velocity

Approach

Ephemeris coordinate-parameterization as a **constrained convex optimization problem**, comparing different surrogate models and approximation intervals

Identified **compliant Chebyshev parameterization** at low data volume for various approximation intervals

Elliptical Lunar Frozen Orbit (ELFO) Scenario

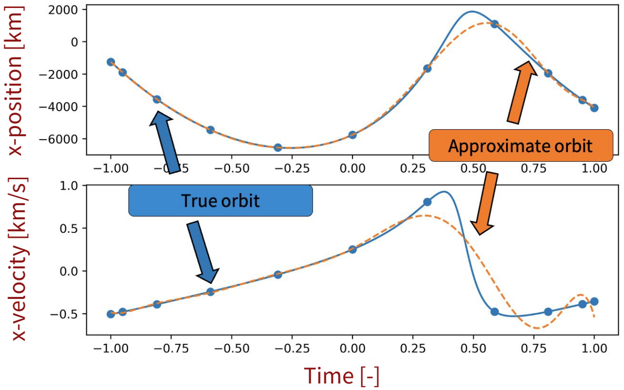

➔ Meet precision requirements

➔ Vary approximation interval

➔ Quantify broadcast message length

Signal-in-Space Error Analysis

	Maximum 3σ $SISE_{pos\,[m]}$	
Approx. Interval	Polynomial	Chebyshev
2 hrs	1.14	1.14
4 hrs	1.41	1.41
8 hrs	3.67	3.67
Requirement	**< 13.34 m (3σ)**	

Message Length

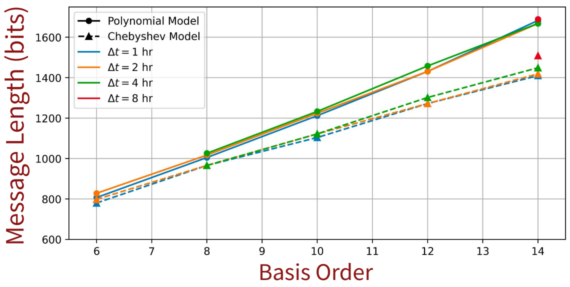

Reference: Cortinovis, M. et al. “Satellite Ephemeris Approximation Methods to Support Lunar Positioning, Navigation, and Timing Services”, *ION GNSS+ 2023, Denver, CO, Sept 2023*

Low Temperature Plasma (LTP) Fluid Moment Modeling

Derek Kuldinow (PhD candidate), Daniel Troyetsky (PhD Candidate), Adnan Mansour (PhD candidate)
Yusuke Yamashita (Postdoc), Kentaro Hara (Advisor)

Developing high-fidelity, robust fluid models for low temperature plasmas in industrial applications

1D/2D Full-Fluid Moment (FFM) Model

- Multifluid model that solves for mass, momentum and energy including inertia, non-neutrality, etc.: Improvement over state-of-the-art, drift-diffusion models in the LTP community
- Applications: Hall effect thrusters [1] and Penning discharge [2]
- Current development: axisymmetric (cylindrical) FFM [3] for industrial applications, e.g., capacitively coupled plasmas (CCPs), spacecraft propulsion, atmospheric-pressure arc discharge

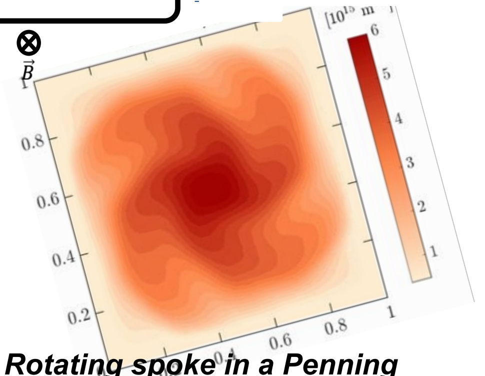

***Rotating spoke in a Penning discharge: Plasma density profile* [2]**

10-Moment Fluid Model

- A fluid approach that models an anisotropic pressure tensor, which can capture kinetic (non-Maxwellian velocity distribution function) effects. cf. Rarefied gas flow
- Applications: shocks, plasma sheaths, discharge [4]
- Goal: Bridge the gap between kinetic (microscopic) and fluid (macroscopic) descriptions of fluid and ionized gases (i.e., plasmas)
- Current development: plasma instabilities, turbulence, cross-field plasma discharges, rarefied gas conditions, laser-plasma interaction

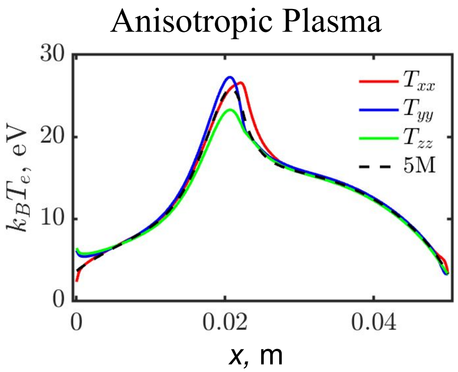

Anisotropic temperature profile inside a Hall-effect thruster

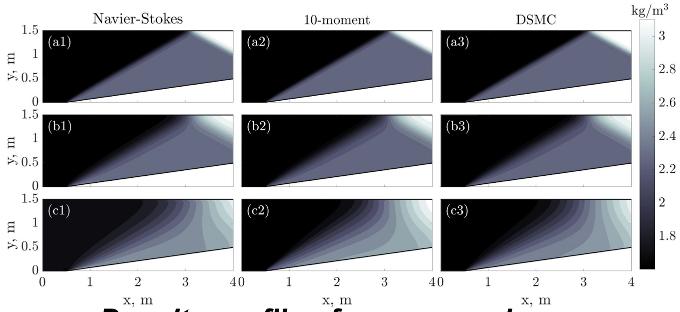

***Density profile of a supersonic ramp with low collisionality* [4]**

References

1: Sahu, Mansour, and Hara, *Phys. Plasmas* **27,** 113505 (2020)
2: Mansour and Hara, *Plasma Source. Sci. Tech.* **31**, 055012 (2022)
3: Mansour and Hara, IEPC-2022-350, June 2022
4: Kuldinow, Mansour, Yamashita, and Hara, *(In Review)*

* Given space considerations, note: Mykel Kochenderfer (mykel@stanford.edu) is the principal investigator for both projects.

Fueled by Purpose: Diffusion and Flattery in Self-Driving

Shounak Ray – B.S. Computer Science
Stanford Intelligent Systems Laboratory (SISL) – Prof. Mykel Kochenderfer

Claims:

Using **diffusion** to generate synthetic driving images **improves object detection.**

(Trained for approximately 48 hours on subset of Waymo and Nuimages Perception Datasets on 2-4 V100 GPUs)

Reverse process of a latent diffusion model trained on street views and traffic scenarios.
Leftmost column shows starting noise and rightmost column presents artificial images.

Dynamically perturbing trajectories of vehicles in **real-world** data *strictly* to maximize reward **improves robustness.**

(A single frame from a particular scenario sourced from the Waymo Motion Dataset)

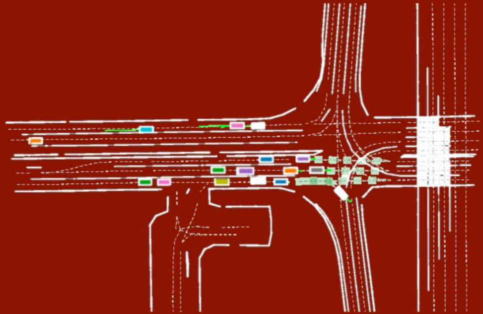

Replay of a single scene from an AV dataset containing real-life vehicle trajectory recordings.
An ego vehicle is set (eg. center orange) and surrounding social trajectories are perturbed.

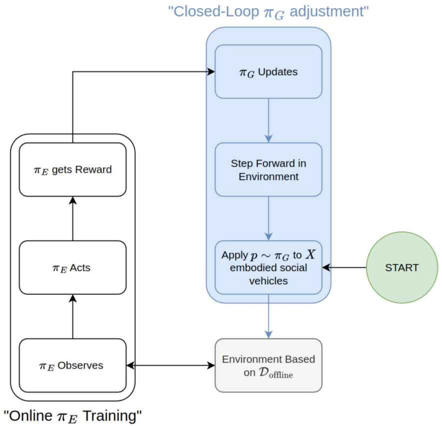

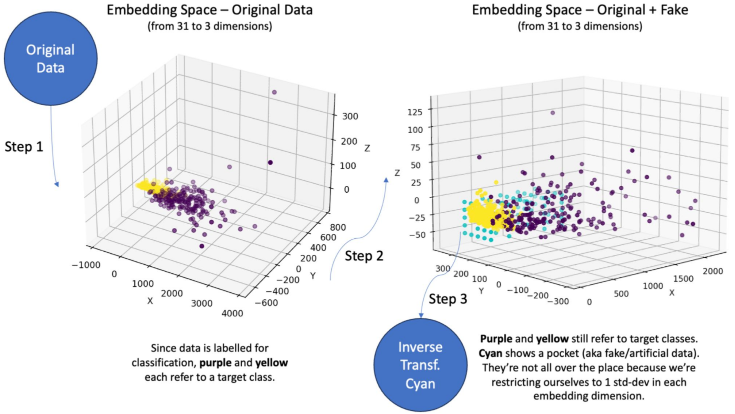

Since data is labelled for classification, **purple** and **yellow** each refer to a target class.

Purple and **yellow** still refer to target classes. **Cyan** shows a pocket (aka fake/artificial data). They're not all over the place because we're restricting ourselves to 1 std-dev in each embedding dimension.

Alboreno Voci
PhD Candidate
Flow Physics & Acoustics Lab
Adivsor: Sanjiva Lele

A high-order, curvilinear multiblock solver using Legion

Alboreno Voci, Mario Di Renzo, Gianluca Iaccarino, Sanjiva Lele
Sanford University, Department of Aeronautics and Astronautics

Introduction

Current experiments targeting rocket propulsion for space/GEO/LEO applications are both expensive and often not as revealing regarding the detailed physics of the process. Thus, scientists turn to computational tools, where the parameters of the problem, operating conditions and uncertainties can be explicitly controlled. The drawbacks of this approach lie in the fact that the computational simulations can sometimes be as expensive as experiments and the credibility of the results is not easily verified.

Purpose of the Work

The goal of this work is to generalize an existing computational simulation framework, HTR[1], so that it can be used for simulations at extreme conditions. Code capabilities include (own contributions in bold)

- **Arbitrary multi-block, curvilinear structured grids**
- High temperature/enthalpy flows with dissociation/ionization
- Multi-material, multi-phase formulation
- Finite rate chemistry computed at runtime
- Integrated uncertainty quantification based on multi-fidelity ensembles
- High performance & scalability using the Legion runtime

Method and Computational Approach

Multi-block simulations (and complex geometries in general for CFD) have been typically used in a finite volume framework. In contrast, finite difference schemes have been used for simpler topologies. Some advances are presented in Meierbachtol[2] et al. Here, a more general treatment for the application of high-order finite difference schemes in arbitrarily connected curvilinear structured grids is presented.
The extension to a regular collection of blocks where the grid points coincide is trivial. Difficulties arise when the connections don't conform in the logical domain. To demonstrate this, a cylindrical pipe domain is considered. The logical representation of the domain involves 4 singularities, or 4 polyjunctions. These singularities require corrections to the implementation of the boundary conditions, viscous & inviscid fluxes. Results are shown for both central and shock capturing schemes.

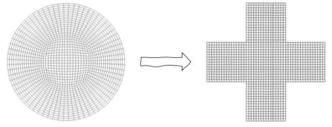

Actual combustor mesh

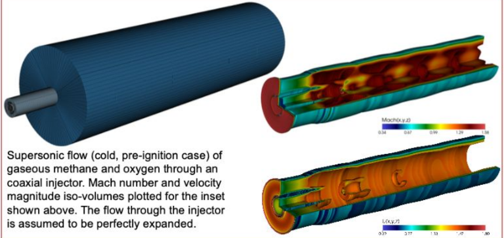

Supersonic flow (cold, pre-ignition case) of gaseous methane and oxygen through an coaxial injector. Mach number and velocity magnitude iso-volumes plotted for the inset shown above. The flow through the injector is assumed to be perfectly expanded.

Verification using canonical problems

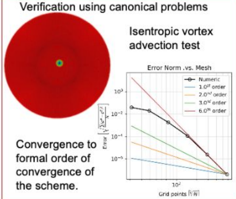

Convergence to formal order of convergence of the scheme.

Weak scaling for different architectures

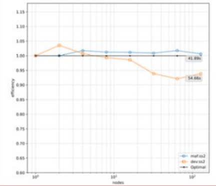

Turbulent pipe flow

Different setups of turbulent flow in a pipe at both subsonic and supersonic Mach number were simulated and the results were compared against previously published DNS data[3]. The vorticity magnitude contours and other QoI don't show contamination from the grid singularities introduced by the mesh.

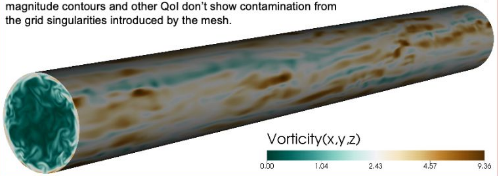

Results

Qualitative and quantitative results are obtained using a variety of verification analytic tests, code-to-code comparisons, and experimental results. All results are found to be in accordance with the expected behavior based on a numerical analysis or within tolerances of measured data. Specifically, turbulence statistics are matched with previously published DNS within 1% in the incompressible case and within 9% for the compressible flow case. The solver maintains robustness when grid singularities are present, and it is shown that the solution is not affected by them.

Turbulence statistics (mean velocity and mean shear stresses) for an incompressible turbulent flow with $Re_b = 5300$, $Re_\tau = 180$, $Ma_b = 0.2$.

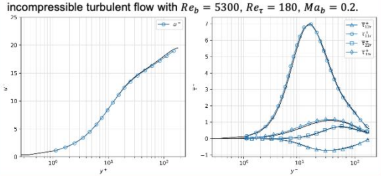

Turbulence statistics (mean velocity and mean shear stresses) for an compressible turbulent flow with $Re_b = 6000$, $Re_\tau = 224$, $Ma_b = 1.5$.

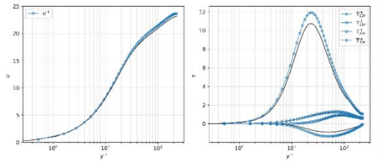

Conclusions

The solver has been verified and validated using canonical flow problems and experimental results. More comprehensive tests of interest, such as flow over a backward facing step, turbulent pipe flow, and coaxial expanding jet. The performance of the solver is also benchmarked on both CPUs/GPUs and found to be satisfactory. Future work consists of large-scale ensembles of laser ignition combustion.

Acknowledgments

This material is based upon work supported by the Department of Energy, National Nuclear Security Administration under Award Number DE-NA0003968.

Bibliography

[1] Di Renzo, M., Fu, L., & Urzay, J. (2020). Computer Physics Communications.
[2] Meierbachtol, Collin S., et al. (2017). J. Comput. Phys.
[3] Modesti, D., & Pirozzoli, S. (2019). Int. J. Fluid Heat Flow.

Further Information

Contact: albovoci@stanford.edu

Semantic Anomaly Detection with Large Language Models

Amine Elhafsi (PhD Candidate) Advisor: Marco Pavone

Stanford University

Autonomous Systems Lab

Semantic Anomalies

Semantic Anomalies: System-level out-of-distribution (OOD) inputs that arise from an unusual or “tricky” combination of individually in-distribution observations.

Real-World Examples:

Stop Sign Imagery on a Billboard

Truck Carrying Traffic Lights

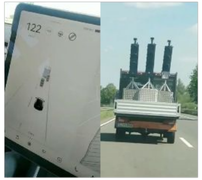

Anomaly Detection Framework

Thanks to the sheer scale of their training datasets, Large Language Model (LLM):

(1) demonstrate **strong automated reasoning performance** and
(2) **possess contextual understanding** in alignment with human intuition.

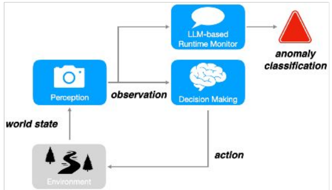

Autonomous Vehicle Monitoring

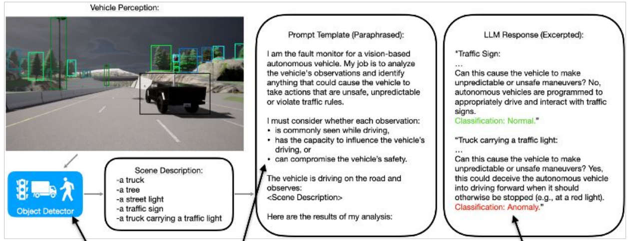

Object detector generates scene description

Chain-of-thought style prompt structures LLM reasoning.

Monitor accurately recognizes the unusual context.

Qualitative Results

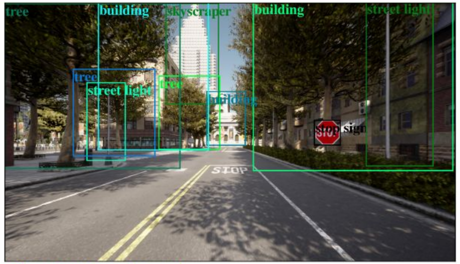

Classification: Normal.

Reasoning: “The vehicle can drive safely in the presence of stop signs.”

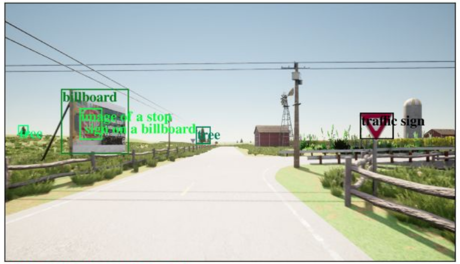

Classification: Anomaly.

Reasoning: “**The autonomous vehicle may mistake the image of the stop sign for an actual stop sign**, which could deceive it into stopping when it should otherwise be driving.”

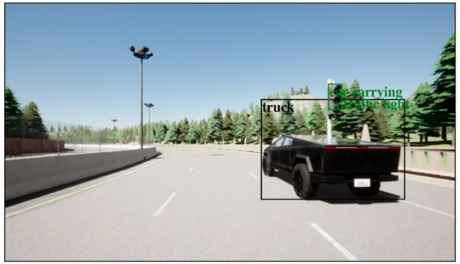

Classification: Anomaly.

Reasoning: “**The autonomous vehicle may mistake the traffic light for a real traffic signal**, which could deceive it into driving forward when it should otherwise be stopped (e.g., at a red light).”

Shape reconstruction of large multi-stable apertures through state sensing

Reconfigurable & Active Structures Lab: Enquan Chew (PhD Candidate), Prof. Maria Sakovsky

Increasingly larger apertures desired for increased performance of space-based phased array antennas

Challenges faced for lightweight architecture
- Thermal and vibration disturbances
- Real time measurement and compensation required

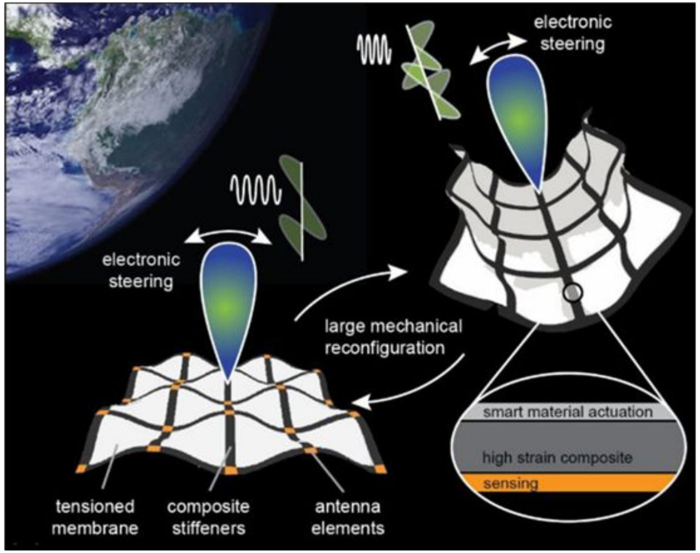

Multi-stable surfaces
- Finite number of discrete stable states

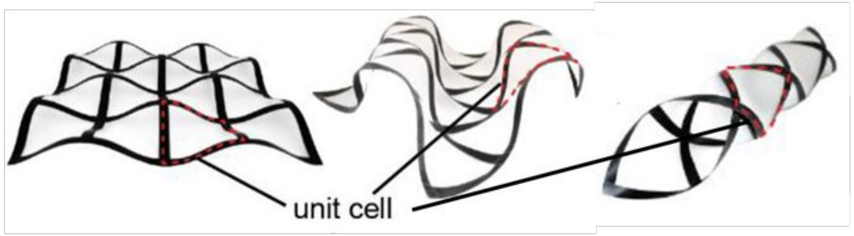

Objective: Realize shape reconstruction of large multi-stable apertures through state sensing

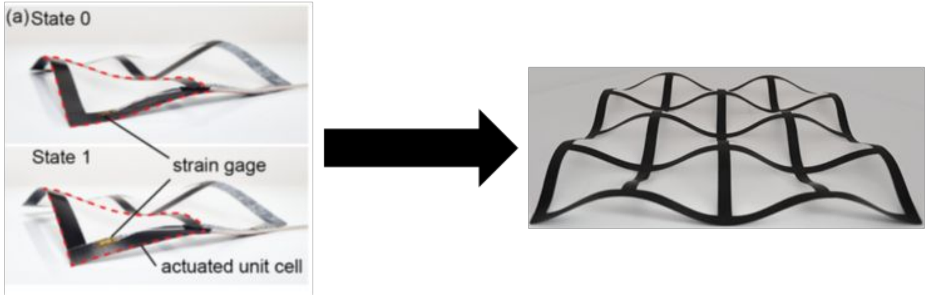

Graphene Aerogel in Microgravity: Electrical Property Characterization

XLab

Synthesizing GA from a graphene hydrogel (GH) starts with a hydrothermal reduction:

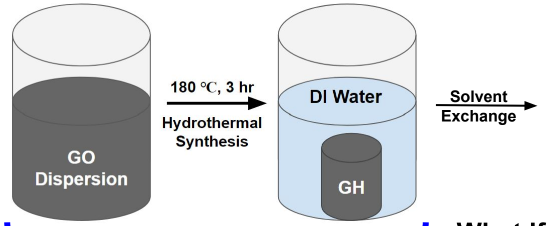

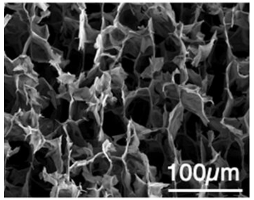

What if we completed this first step in space?

Earth-synthesized graphene aerogel

- Buoyancy induced effects
- Sedimentation & stratification
- Anisotropic properties

Microgravity-synthesized graphene aerogel

- Brownian motion driven effects
- More uniform microstructure
- Isotropic properties

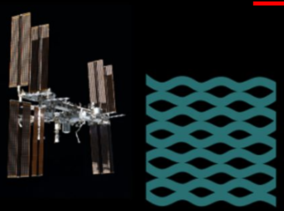

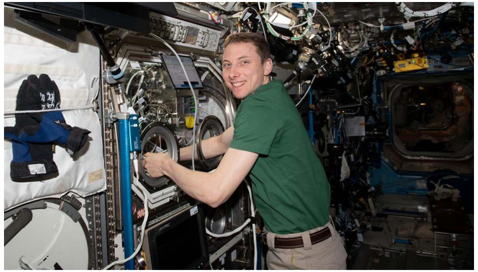

Image courtesy of NASA

Astronaut Woody Hoburg completing our experiment!

Preliminary Electrical Characterization: van der Pauw Method

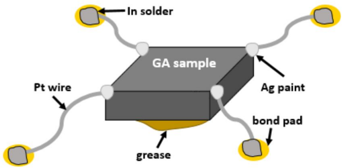

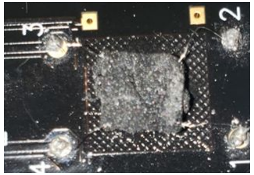

Current/Future Electrical Characterization: Electrochemical

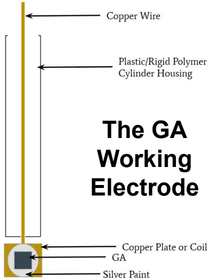

The GA Working Electrode

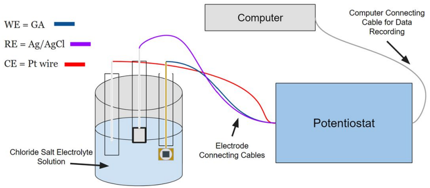

Applications

- ➔ Sensor technology
- ➔ Capacitors and batteries
- ➔ EM wave absorption
- ➔ Thermal insulation for spacecraft

Synthesis Hardware on the ISS

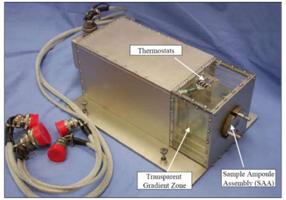

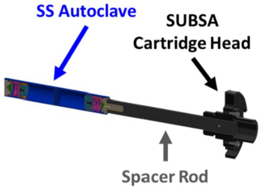

NASA's SUBSA (solidification using a baffle in sealed ampoules) furnace managed by Techshot, Inc., a Redwire Company.

NSF
Berkeley UNIVERSITY OF CALIFORNIA
ISS U.S. NATIONAL LABORATORY
REDWIRE

Detecting Space Based Interference on GNSS Signals

Akshata Patil, R. Eric Phelts, Yu-Hsuan Chen, Sherman Lo, Todd Walter